

A possibility of a protein-bound water molecule as the ionizable group responsible for pK_e at the alkaline side in human matrix metalloproteinase 7 activity

Received November 30, 2011; accepted January 9, 2012; published online February 24, 2012

Aiko Morishima, Kiyoshi Yasukawa and Kuniyo Inouye*

Division of Food Science and Biotechnology, Graduate School of Agriculture, Kyoto University, Sakyo-ku, Kyoto 606-8502, Japan

*Kuniyo Inouye, Division of Food Science and Biotechnology, Graduate School of Agriculture, Kyoto University, Sakyo-ku, Kyoto 606 8502, Japan. Tel: +81 75 753 6266, Fax: +81 75 753 6265, email: inouye@kais.kyoto-u.ac.jp

Human matrix metalloproteinase 7 (MMP-7) activity exhibits broad bell-shaped pH profile with the acidic and alkaline pK_a (pK_{e1} and pK_{e2}) values of about 4 and 10. The ionizable group for pK_{e2} was assigned to Lys or Arg by thermodynamic analysis; however, no such residues are present in the active site. Hence, based on the crystal structure, we hypothesized that a water molecule bound to the main-chain nitrogen of Ala162 (W1) or the main-chain carbonyl oxygen of Pro217 (W2) is a candidate for the ionizable group for pK_{e2} [Takeharu, H. *et al.* (2011) *Biochim. Biophys. Acta* 1814, 1940–1946]. In this study, we inspected this hypothesis. In the hydrolysis of (7-methoxycoumarin-4-yl)acetyl-L-Pro-L-Leu-Gly-L-Leu-[N^3 -(2,4-dinitrophenyl)-L-2,3-diaminopropionyl]-L-Ala-L-Arg-NH₂, all 19 variants, in which one of all Lys and Arg residues was replaced by Ala, retained activity, indicating that neither Lys nor Arg is the ionizable group. pK_{e2} values of A162S, A162V and A162G were 9.6 ± 0.1 , 9.5 ± 0.1 and 10.4 ± 0.2 , respectively, different from that of wild-type MMP-7 (WT) (9.9 ± 0.1) by 0.3–0.5 pH unit, and those of P217S, P217V and P217G were 10.1 ± 0.1 , 9.8 ± 0.1 and 9.7 ± 0.1 , respectively, different from that of WT by 0.1–0.2 pH unit. These results suggest a possibility of W1 or W2 as the ionizable group for pK_{e2} .

Keywords: ionizable group/matrix metalloproteinase/matrix metalloproteinase (MMP)-7; site-directed mutagenesis/water molecule.

Abbreviations: AMPSO, 3-[(1,1-dimethyl-2-hydroxyethyl) amino]-2-hydroxypropane sulphonic acid; DMSO, dimethyl sulphoxide; HEPES, 2-[4-(2-hydroxyethyl)-1-piperazinyl] ethanesulphonic acid; K_e , proton dissociation constant; MES, 2-(*N*-morpholino)ethanesulphonic acid; MMP, matrix metalloproteinase; MOCAC-PLG, (7-methoxycoumarin-4-yl)acetyl-L-Pro-L-Leu-Gly; MOCAC-PLGL(Dpa)AR, (7-methoxycoumarin-4-yl)

acetyl-L-Pro-L-Leu-Gly-L-Leu-[N^3 -(2,4-dinitrophenyl)-L-2,3-diaminopropionyl]-L-Ala-L-Arg-NH₂.

Human matrix metalloproteinase 7 (MMP-7, matrilysin) [EC 3.4.24.23] is one of the smallest matrix metalloproteinases (MMP) (1). Almost all MMPs consist of a prodomain, a catalytic domain, a hinge region and a haemopexin domain, but MMP-7 lacks a hinge region and a haemopexin domain. MMP-7 is activated automatically by removal of the prodomain. It is thought to play important roles in tumour invasion and metastasis (1). The molecular mass of the latent pro-form of MMP-7 is 28 kDa, and that of the mature form is 19 kDa (2). According to X-ray crystallography, MMP-7 consists of three α -helices and a five-stranded β -sheet, and contains a zinc ion, essential for activity and other zinc ion and two calcium ions that are thought necessary for stability (Fig. 1A) (3). All MMP family enzymes have a consensus sequence HEXXHXXGXXH and methionine-containing turn (Met-turn), and are grouped in clan MA(M), in which three histidine residues chelate a catalytic zinc ion (4). We have reported inhibitory effects of alcohols (5, 6), synthetic MMP inhibitors thiorphan and R-94138 (7), lignans (8) and green tea catechins (9, 10).

Generally, ionizable groups involved in the catalytic mechanism of enzyme are estimated from the 3D structure and pK_a values. MMP-7 exhibits broad bell-shaped profile of the pH-dependence. The acidic and alkaline pK_a (pK_{e1} and pK_{e2}) values are about 4 and 10 (In this study, the pK_a of the ionizable group of MMP-7 is designated pK_e , and the suffixes 1 and 2 indicate that the respective pK_a 's are on the acidic and alkaline side, respectively) (7, 11). As a result, Glu198 and Tyr219 (In this study, the numbering of amino acid residues of pro-MMP-7 (12) is used, in which the mature MMP-7 begins at Tyr78) were thought for ionizable groups responsible for pK_{e1} and pK_{e2} , respectively (7, 11, 13). We demonstrated that neither nitration of the tyrosyl residues (14) nor the mutations of active-site tyrosyl residues (Tyr193, Tyr216, or Tyr219) (15) abolished the activity. No other residues that could be candidates for the ionizable group for pK_{e2} are located in the active site.

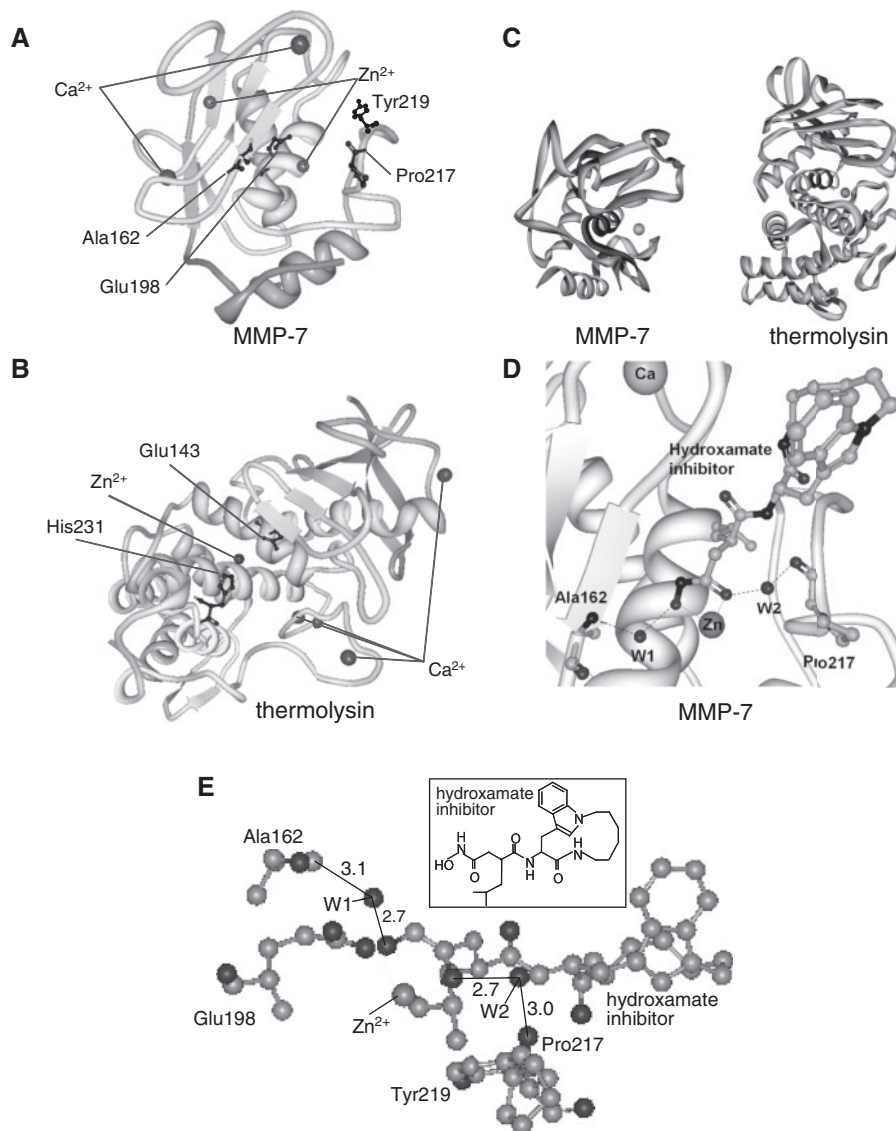


Fig. 1 3D structure. The MMP-7 and thermolysin structures are based on the Protein Data Bank accession nos. 1MMQ and 8TLN, respectively. Peptide chain is represented by ribbon (A–D) and ball and stick (E) models. Zn^{2+} and Ca^{2+} are shown as a sphere. (A) Whole structure of MMP-7. A catalytically important residue, Glu198, and residues subjected to mutation, Ala162 and Pro217, and Tyr219 are shown as ball and stick. (B) Whole structure of thermolysin. Catalytically important residues, Glu143 and His231, are shown as ball and stick. (C) Comparison of MMP-7 and thermolysin. The consensus zinc-binding sequences HEXXHXXGXXH in MMP-7 and HEXXH in thermolysin are shown as filled ribbon. (A–C) The catalytic Zn^{2+} is shown as a sphere. (D and E) Close-up view of the active site of MMP-7. (D) Ala162, Pro217 and the hydroxamate inhibitor are shown as ball and stick. (E) The catalytic Zn^{2+} , two water molecules (W1 and W2), the hydroxamate inhibitor, and the main and side chains of Ala162, Glu198, Pro217 and Tyr219 are shown as ball and stick. The number indicates the distance (Å).

Under these backgrounds, we previously made thermodynamic analysis. pK_a of side chains of six amino acids (L-Asp, L-Glu, L-His, L-Cys, L-Tyr, L-Lys and L-Arg) at 25–45°C were determined by the pH titration of amino-acid solutions, and their enthalpy changes, ΔH° , of deprotonation were calculated and used for the estimation of the ionizable groups of MMP-7 (16). The ionizable group for pK_{e1} was assigned to Asp or Glu, and that for pK_{e2} was to Lys or Arg, suggesting that Glu198 in the active site is the ionizable group for pK_{e1} (16). However, no Lys or Arg residues are present in the active site. The hydroxamate (–CO–NHOH) peptide mimetic inhibitor, which binds covalently to the active-site zinc ion, is the first MMP inhibitor (17). In the complex of MMP-7 and this

inhibitor (Protein Data Bank no. 1MMQ) (3), we have noticed two water molecules (W1 and W2) (Fig. 1D and E), and have hypothesized that W1 or W2 is the ionizable group responsible for pK_{e2} due to the following reasons (16). (i) Both W1 and W2 are located 2.7 Å far from one of the two oxygen atoms of hydroxamate that bind with the active site zinc ion; (ii) the atoms to which W1 and W2 bind are the main-chain nitrogen of Ala162 and the main-chain carbonyl oxygen of Pro217, respectively. Ala162, located in the fourth β -sheet (Ala162–Ala164), and Pro 217, located in the Met-turn (Pro211–Gly222), are conserved among MMPs; and (iii) water molecules corresponding to W1 and W2 are also found in the X-ray crystallographic structures of MMP-7 complexed with

a carboxylate inhibitor (1MMP) and a sulphodiimine inhibitor (1MMR) (3).

In this study, we explored the possibility of W1 and W2 as the ionizable group responsible for pK_{e2} of MMP-7. For this purpose, we made thermodynamic and site-directed mutagenesis analyses. In the thermodynamic analysis, we used thermolysin [EC 3.4.24.27] for comparison. Thermolysin is a representative thermostable neutral zinc metalloproteinase from *Bacillus thermoproteolyticus*. It has a consensus sequence HEXXH and is grouped in MA(E) (18). It requires one zinc ion for enzyme activity and four calcium ions for structural stability, and consists of 316 amino acid residues (Fig. 1B). In MMP-7, the active-site lies in the shallow cleft, whereas in thermolysin, it lies in the deep cleft (Fig. 1C). Thermolysin exhibits bell-shaped profile of the pH dependence with pK_{e1} and pK_{e2} values of about 5 and 8 (19–23). As a result, Glu143 (21) and the zinc-bound water (22, 23) have been thought for ionizable groups responsible for pK_{e1} , and His 231 has been thought for that for pK_{e2} (21–23). In this study, we also discuss the usefulness of the present method, a combination of thermodynamic analysis and site-directed mutagenesis analysis, for the estimation of ionizable groups in the catalytic mechanism of enzyme.

Materials and Methods

Materials

(7-Methoxycoumarin-4-yl)acetyl-L-Pro-L-Leu-Gly-L-Leu-[N^3 -(2,4-dinitrophenyl)-L-2,3-diaminopropionyl]-L-Ala-L-Arg-NH₂. [MOCAC-PLGL(Dpa)AR] (lot no. 491214, molecular mass

1093.2 Da) (24) and (7-methoxycoumarin-4-yl)acetyl-L-Pro-L-Leu-Gly (MOCAC-PLG) (lot no. 510913, 501.54 Da) were purchased from the Peptide Institute (Osaka, Japan). Their concentrations were determined by the denoted weights and the molecule masses. 3-[(1,1-Dimethyl-2-hydroxy-ethyl)amino]-2-hydroxypropane sulphonic acid (AMPSO) was from Wako Pure Chemical (Osaka). Thermolysin produced from the culture broth of *Bacillus thermoproteolyticus* (8,720 proteinase units mg^{-1} according to the supplier) was from Daiwa Kasei (Osaka). On SDS-PAGE under reducing conditions, it yielded single bands with a molecular mass of 36 kDa (lane 3 in Fig. 2A). All other chemicals were from Nacalai Tesque (Kyoto, Japan).

Expression and purification of MMP-7

Expression in *Escherichia coli* and purification of recombinant MMP-7 were carried out as described previously (25, 26). Briefly, mature MMP-7 (Tyr78–Lys250) was expressed in BL21(DE3) cells in the form of inclusion bodies, from which solubilized with 6 M guanidine HCl, refolded with 1 M L-arginine, and purified by ammonium sulphate precipitation and heparin affinity column-chromatography. On SDS-PAGE under reducing conditions, the purified preparation of wild-type MMP-7 (WT) yielded single bands with a molecular mass of 19 kDa (lane 2 in Fig. 2A). The concentration of MMP-7 was determined spectrophotometrically using a molar absorption coefficient at 280 nm, ϵ_{280} , of 31,800 $M^{-1}cm^{-1}$ (27). Site-directed mutagenesis was carried out using Quikchange™ site-directed mutagenesis kit (Stratagene, La Jolla, CA, USA). The nucleotide sequences of mutated MMP-7 genes were verified by a Shimadzu DNA sequencer DSQ-2000 (Shimadzu, Kyoto). SDS-PAGE was performed in a 12.5% polyacrylamide gel under reducing conditions by the method of Laemmli (28).

Fluorometric analysis of hydrolysis of MOCAC-PLGL(Dpa)AR

The MMP-7-catalysed hydrolysis of MOCAC-PLGL(Dpa)AR was initiated by mixing 2,444 μl of the reaction buffer, 40 μl of MMP-7 solution (625 nM) and 16 μl of the substrate solution (234 μM) dissolved in DMSO. The initial concentrations of enzyme and MOCAC-PLGL(Dpa)AR were 10 nM and 1.5 μM , respectively. The reaction

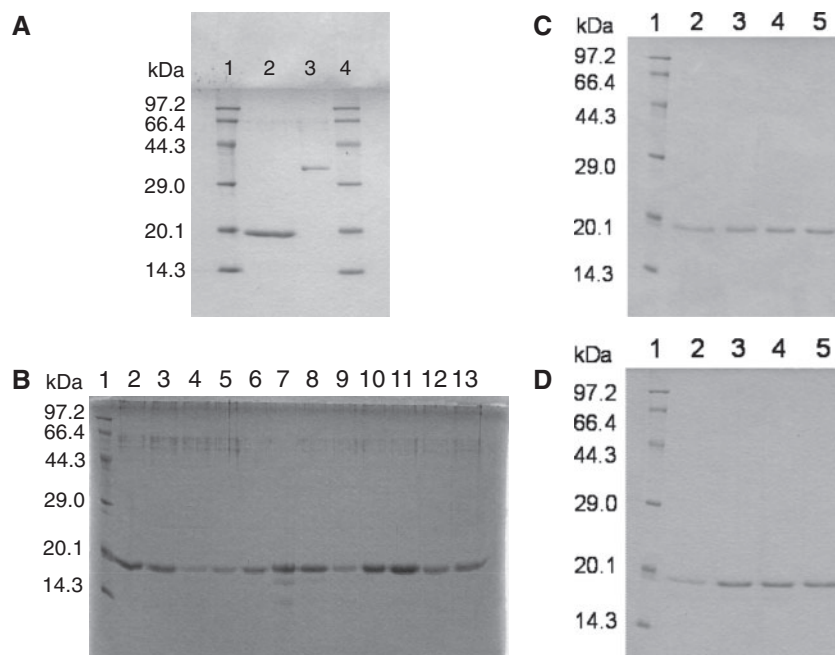


Fig. 2 SDS-PAGE under reducing conditions. Coomassie brilliant blue-stained 12.5% SDS-polyacrylamide gel is shown. (A) Wild-type MMP-7 and thermolysin. Lane 1, molecular-mass marker; lane 2, MMP-7; and lane 3, thermolysin. (B) MMP-7 variants in which single Lys residue was replaced by Ala. Lane 1, molecular-mass marker; lane 2, wild-type MMP-7; lane 3, K86A; lane 4, K90A; lane 5, K114A; lane 6, K121A; lane 7, K129A; lane 8, K228A; lane 9, K235A; lane 10, K239A; lane 11, K243A; lane 12, K249A; and lane 13, K250A. (C) MMP-7 variants of Ala 162. Lane 1, molecular mass marker; lane 2, wild-type MMP-7; lane 3, A162S; lane 4, A162V; and lane 5, A162G. (D) MMP-7 variants of Pro 217. Lane 1, molecular-mass marker; lane 2, wild-type MMP-7; lane 3, P217S; lane 4, P217V; and lane 5, P217G.

buffers were 50 mM acetate–NaOH buffer at pH 3.6–5.6, 50 mM MES–NaOH buffer at pH 5.4–7.2, 50 mM HEPES–NaOH buffer at pH 7.0–8.8 and 50 mM AMPSO–NaOH buffer at pH 8.6–10.4, each containing 10 mM CaCl₂. All buffers were prepared at 15, 25, 35 and 45°C, respectively. The reaction was measured by following the increase in fluorescence intensity at 393 nm with excitation at 328 nm with a Shimadzu RF-5300 fluorescence spectrophotometer. The peptide bond between Gly and L-Leu residues was cleaved by MMP-7, and the amount of MOCAC-PLG was estimated by fluorescence intensity by comparison with that of the MOCAC-PLG solution. Since the initial concentration of MOCAC-PLGL(Dpa)AR (1.5 μM) is much lower than the Michaelis constant (K_m) (30 μM) (5–9), the hydrolysis was carried out under pseudo first-order conditions. The Michaelis–Menten equation was expressed as $v_o = (k_{cat}/K_m)[E]_o[S]_o$, where v_o , k_{cat} , $[E]_o$ and $[S]_o$ are the initial reaction rate, the molecular activity, the initial enzyme concentration, and the initial substrate concentration, respectively. The intrinsic k_{cat}/K_m ($(k_{cat}/K_m)_o$) and the proton dissociation constants (K_{e1} and K_{e2}) for the bell-shaped pH dependence of the activity (k_{cat}/K_m) were calculated from Eq. (1) by a non-linear least squares regression method with Kaleida Graph Version 3.5 (Synergy Software, Essex, VT, USA):

$$(k_{cat}/K_m)_{obs} = \frac{(k_{cat}/K_m)_o}{1 + \frac{[H]}{K_{e1}} + \frac{K_{e2}}{[H]}} \quad (1)$$

In this equation, $(k_{cat}/K_m)_{obs}$ and $[H]$ are the k_{cat}/K_m value observed and the proton concentration, respectively, at a specified pH.

Results

Effects of pH on the activities of MMP-7 and thermolysin

The pH dependence of k_{cat}/K_m of MMP-7 and thermolysin was examined in the range of pH 3.6–10.4 at 15, 25, 35 and 45°C (Fig. 3). Both enzymes exhibited bell-shaped profiles at all temperatures. The catalytically optimal pH ranges were 5.5–8.5 in MMP-7 and 6.0–7.5 in thermolysin. In MMP-7, the plot at 15°C showed the widest active pH range and that at 45°C the narrowest. In thermolysin, all plots showed similar active pH ranges. The pK_{e1} , pK_{e2} and $(k_{cat}/K_m)_o$ at each temperature are summarized in Table I. The $(k_{cat}/K_m)_o$ value of MMP-7 increased with increasing temperature at 15–45°C, while that of thermolysin reached maximum at 25°C. We confirmed that no significant conformational change was occurred in the enzymes by the changes in pH and temperature by the CD measurement at 200–270 nm (data not shown).

Figure 4 shows van't Hoff plots for pK_{e1} and pK_{e2} . The standard enthalpy change, ΔH° , of the deprotonation was calculated from the slope to be $-11 \pm 6 \text{ kJ mol}^{-1}$ for pK_{e1} and $76 \pm 19 \text{ kJ mol}^{-1}$ for pK_{e2} of MMP-7, which agreed well with the values in our previous reports ($-21 \pm 6 \text{ kJ mol}^{-1}$ for pK_{e1} and $90 \pm 4 \text{ kJ mol}^{-1}$ for pK_{e2}) (16) and $-4.2 \pm 3.2 \text{ kJ mol}^{-1}$ for pK_{e1} and $29 \pm 1 \text{ kJ mol}^{-1}$ for pK_{e2} of thermolysin. By comparison with ΔH° of deprotonation of the side chains of free amino acids, L-Asp ($-6.4 \pm 3.5 \text{ kJ mol}^{-1}$), L-Glu ($-24 \pm 6 \text{ kJ mol}^{-1}$), L-His ($27 \pm 6 \text{ kJ mol}^{-1}$), L-Cys ($28 \pm 2 \text{ kJ mol}^{-1}$), L-Tyr ($52 \pm 9 \text{ kJ mol}^{-1}$), L-Arg ($70 \pm 4 \text{ kJ mol}^{-1}$) and N^α -acetyl-L-Lys ($88 \pm 6 \text{ kJ mol}^{-1}$) (16), the ionizable groups of MMP-7 were assigned to Asp or Glu for pK_{e1} and Lys or Arg for pK_{e2} , and those of thermolysin were assigned to Asp or Glu for pK_{e1} and Tyr, Cys or His for pK_{e2} . Therefore, in MMP-7, the ionizable group for pK_{e1} was assigned

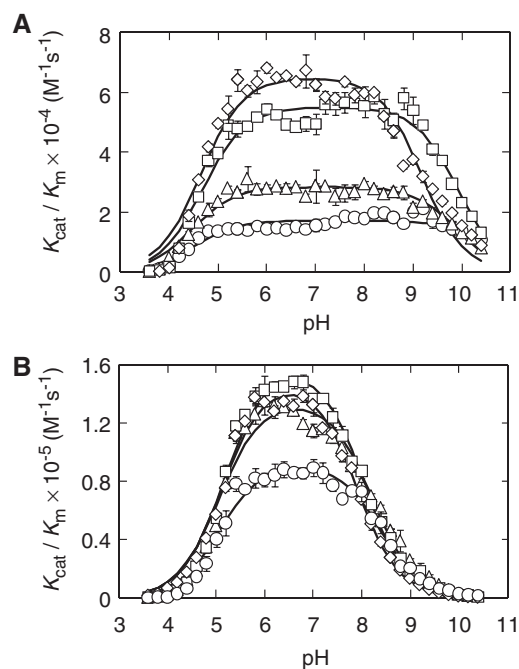


Fig. 3 Effects of pH on the MOCAC-PLGL(Dpa)AR-hydrolysis activities of MMP-7 and thermolysin. (A) MMP-7. (B) thermolysin. Temperatures: 15°C (open circle); 25°C (open triangle); 35°C (open square); and 45°C (open diamond). Error bars indicate SD value. Solid lines were drawn by best-fitting the data to Equation (1).

Table I. pK_e values and intrinsic k_{cat}/K_m ($(k_{cat}/K_m)_o$) of MMP-7 and thermolysin in the hydrolysis of MOCAC-PLGL(Dpa)AR.

Temperature (°C)	pK_{e1}	pK_{e2}	$(k_{cat}/K_m)_o \times 10^{-4}$ ($M^{-1} s^{-1}$)
MMP-7			
15	4.5 ± 0.1	10.6 ± 0.1	1.7 ± 0.1
25	4.5 ± 0.1	9.9 ± 0.1	2.8 ± 0.1
35	4.7 ± 0.1	9.9 ± 0.1	5.5 ± 0.1
45	4.7 ± 0.1	9.2 ± 0.1	6.5 ± 0.2
Temperature (°C)	pK_{e1}	pK_{e2}	$(k_{cat}/K_m)_o \times 10^{-5}$ ($M^{-1} s^{-1}$)
Thermolysin			
15	5.1 ± 0.1	8.4 ± 0.1	0.9 ± 0.1
25	5.1 ± 0.1	8.2 ± 0.1	1.4 ± 0.1
35	5.2 ± 0.5	8.0 ± 0.1	1.6 ± 0.1
45	5.1 ± 0.0	7.9 ± 0.1	1.5 ± 0.1

to Glu198 in the active site, but that for pK_{e2} could not be assigned to any residues because no Lys or Arg residues are present in the active site, as reported previously (19). In thermolysin, the ionizable groups for pK_{e1} and pK_{e2} were assigned to Glu143 and His231 in the active site, respectively, which agreed well with the previous report (22).

Effects of the mutations of Lys and Arg residues on MMP-7 activity

MMP-7 has 11 Lys residues and 8 Arg residues. To exclude the possibility that one or some of them plays an important role in catalysis, 11 variants in which one of Lys residues was replaced by Ala (K86A, K90A,

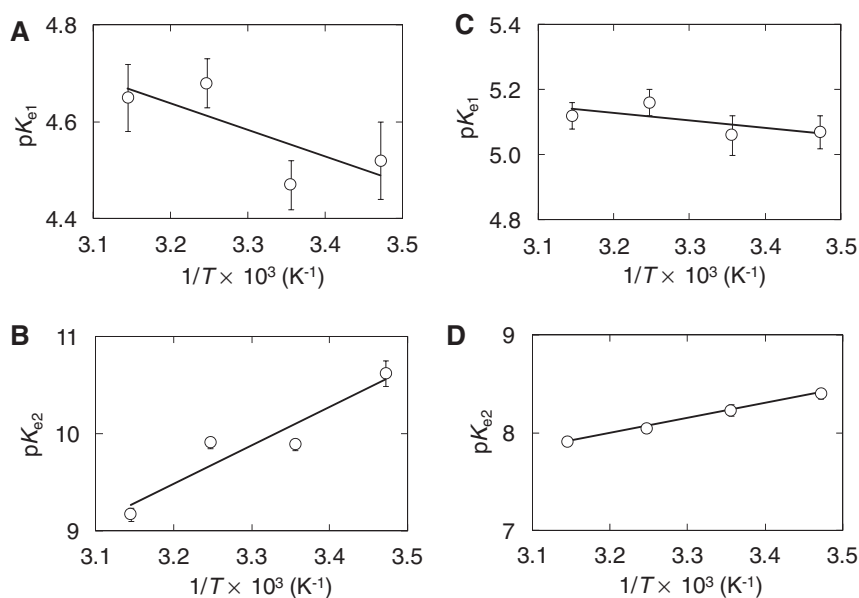


Fig. 4 van't Hoff plot. (A) pK_{e1} of MMP-7. (B) pK_{e2} of MMP-7. (C) pK_{e1} of thermolysin. (D) pK_{e2} of thermolysin. Error bars indicate SD value. Enthalpy change, ΔH° , of deprotonation was calculated from the slope to be $-11 \pm 6 \text{ kJ mol}^{-1}$ (A), $76 \pm 19 \text{ kJ mol}^{-1}$ (B), $-4.2 \pm 3.2 \text{ kJ mol}^{-1}$ (C) and $29 \pm 1 \text{ kJ mol}^{-1}$ (D).

K114A, K121A, K129A, K228A, K235A, K239A, K243A, K249A and K250A) and 8 variants in which 1 of Arg residues was replaced by Ala (R95A, R101A, R110A, R128A, R143A, R180A, R244A and R248A) were designed. They were expressed in *E. coli* and purified. On SDS-PAGE under reducing conditions, purified preparation of Lys- (Fig. 2B) and Arg residue variants (data not shown) yielded a single band with a molecular mass of 19 kDa. Table II shows k_{cat}/K_m of the variants in the hydrolysis of MOCac-PLGL(Dpa)AR at pH 7.5 at 25°C. All variants had activity although the k_{cat}/K_m values differed among variants in the range of 2–265% of that of WT. These results indicate that neither Lys nor Arg residue is the ionizable group responsible for pK_{e2} , suggesting that a protein-bound water could be the ionizable group for pK_{e2} .

We assumed that if a water molecule bound to the main-chain nitrogen of Ala162 (W1) or a water molecule bound to the main-chain carbonyl oxygen of Pro217 (W2) is the ionizable group for pK_{e2} , the mutations of Ala162 or Pro217 do not abolish the activity but affect it significantly. Nine Ala162 variants: A162S, A162V, A162G, A162T, A162L, A162K, A162P, A162C and A162E and nine Pro217 variants: P217S, P217V, P217G, P217T, P217L, P217K, P217C, P217E and P217D were designed, expressed in *E. coli*, and purified. On SDS-PAGE under reducing conditions, purified preparations yielded a single band with a molecular mass of 19 kDa (Fig. 2C for A162S, A162V and A162G; Fig. 2D for P217S, P217V and P217G; data not shown for other variants). Table II shows the k_{cat}/K_m values of the variants in the hydrolysis of MOCac-PLGL(Dpa)AR at pH 7.5 at 25°C. A162P lacked the activity. The k_{cat}/K_m values of the other eight Ala162 variants were in the range of 1–193% of that of WT, and those of the nine Pro217

Table II. k_{cat}/K_m of MMP-7 variants in the hydrolysis of MOCac-PLGL(Dpa)AR at pH 7.5, at 25°C.

MMP-7	$k_{cat}/K_m \times 10^{-4} (\text{M}^{-1} \text{s}^{-1})$
WT	2.53 ± 0.29 (1.00)
K86A	3.05 ± 0.25 (1.20)
K90A	1.14 ± 0.12 (0.45)
K114A	0.19 ± 0.01 (0.08)
K121A	0.39 ± 0.06 (0.15)
K129A	0.32 ± 0.02 (0.13)
K228A	0.66 ± 0.06 (0.26)
K235A	3.71 ± 0.73 (1.47)
K239A	6.71 ± 0.10 (2.65)
K243A	3.51 ± 0.04 (1.39)
K249A	5.82 ± 0.39 (2.30)
K250A	4.19 ± 0.02 (1.65)
R95A	0.05 ± 0.02 (0.02)
R101A	2.40 ± 0.19 (0.95)
R110A	2.76 ± 0.10 (1.09)
R128A	0.65 ± 0.04 (0.26)
R143A	2.93 ± 0.04 (1.16)
R180A	2.15 ± 0.06 (0.85)
R244A	6.24 ± 0.73 (2.47)
R248A	5.10 ± 0.03 (2.02)
A162S	4.83 ± 0.25 (1.91)
A162V	0.59 ± 0.01 (0.23)
A162G	2.84 ± 0.26 (1.12)
A162T	1.69 ± 0.04 (0.67)
A162L	1.16 ± 0.02 (0.46)
A162K	0.03 ± 0.01 (0.01)
A162P	ND ^a
A162C	4.90 ± 0.84 (1.93)
A162E	0.03 ± 0.01 (0.01)
P217S	6.74 ± 0.29 (2.66)
P217V	1.64 ± 0.20 (0.65)
P217G	4.59 ± 0.05 (1.81)
P217T	3.93 ± 0.70 (1.55)
P217L	2.25 ± 0.04 (0.89)
P217K	1.39 ± 0.47 (0.55)
P217C	2.74 ± 0.30 (1.08)
P217E	3.70 ± 0.04 (1.46)
P217D	3.94 ± 0.28 (1.56)

Numbers in parentheses indicate relative k_{cat}/K_m values compared to that of WT.

^aND, not detectable.

variants were in the range of 55–266% of that of WT. This indicates that mutation of Ala162 and that of Pro217 do not abolish the activity (except for that of Ala162 into Pro) but affect it in a considerable degree.

Effects of the mutations of Ala162 and Pro217 on MMP-7 activity

From the Ala162 and Pro217 variants constructed, we selected three Ala162 variants: A162S, A162V and A162G and three Pro217 variants: P217S, P217V and P217G, and examined their pH dependence of the $k_{\text{cat}}/K_{\text{m}}$ values in the hydrolysis of MOCac-PLGL(Dpa)AR at 25°C. A162S and P217S were selected because they might lack the hydrophobic character at the amino acid position of 162 and 217, respectively. A162V and P217V were selected because they might have increased hydrophobicity at the position. A162G and P217G were selected because they might have increased flexibility of the main chain at the position. All variants exhibited bell-shaped pH-dependence profiles of the activity (Fig. 5A and B). The kinetic parameters are summarized in Table III. The $\text{p}K_{\text{e}2}$ values of A162S, A162V and A162G were 9.6 ± 0.1 , 9.5 ± 0.2 and 10.4 ± 0.2 , respectively, different from that of WT (9.9 ± 0.1) by

0.3–0.5 pH unit. The $\text{p}K_{\text{e}2}$ values of P217S, P217V and P217G were 10.1 ± 0.1 , 9.8 ± 0.1 and 9.7 ± 0.1 , respectively, different from that of WT by 0.1–0.2 pH unit. Figure 5C–E shows the normalized pH-dependence curves. At pH around the $\text{p}K_{\text{e}2}$ value of WT (9.9), the profiles of Ala162 variants (broken lines) were more different from that of WT than those of Pro217 variants (dotted lines), indicating that the mutations of Ala162 give larger effects on $\text{p}K_{\text{e}2}$ than those of Pro217.

Table III. $\text{p}K_{\text{e}}$ values and intrinsic $k_{\text{cat}}/K_{\text{m}}$ [$(k_{\text{cat}}/K_{\text{m}})_0$] of MMP-7 variants in the hydrolysis of MOCac-PLGL(Dpa)AR at 25°C.

MMP-7	$\text{p}K_{\text{e}1}$	$\text{p}K_{\text{e}2}$	$(k_{\text{cat}}/K_{\text{m}})_0 \times 10^{-4}$ ($\text{M}^{-1} \text{s}^{-1}$)
WT	4.6 ± 0.1 (0)	9.9 ± 0.1 (0)	2.9 ± 0.1 (1.0)
A162S	4.7 ± 0.1 (+0.1)	9.6 ± 0.1 (−0.3)	6.4 ± 0.3 (2.2)
A162V	4.6 ± 0.2 (+0.0)	9.5 ± 0.2 (−0.4)	0.6 ± 0.0 (0.2)
A162G	4.4 ± 0.1 (−0.2)	10.4 ± 0.2 (+0.5)	2.9 ± 0.1 (1.0)
P217S	4.8 ± 0.1 (+0.2)	10.1 ± 0.1 (+0.2)	5.4 ± 0.2 (1.8)
P217V	4.6 ± 0.1 (+0.0)	9.8 ± 0.1 (−0.1)	1.7 ± 0.1 (0.6)
P217G	4.9 ± 0.1 (+0.3)	9.7 ± 0.1 (−0.2)	4.7 ± 0.1 (1.6)

Numbers in parentheses indicate $\Delta \text{p}K_{\text{e}}$ compared to WT and $k_{\text{cat}}/K_{\text{m}}$ relative to WT.

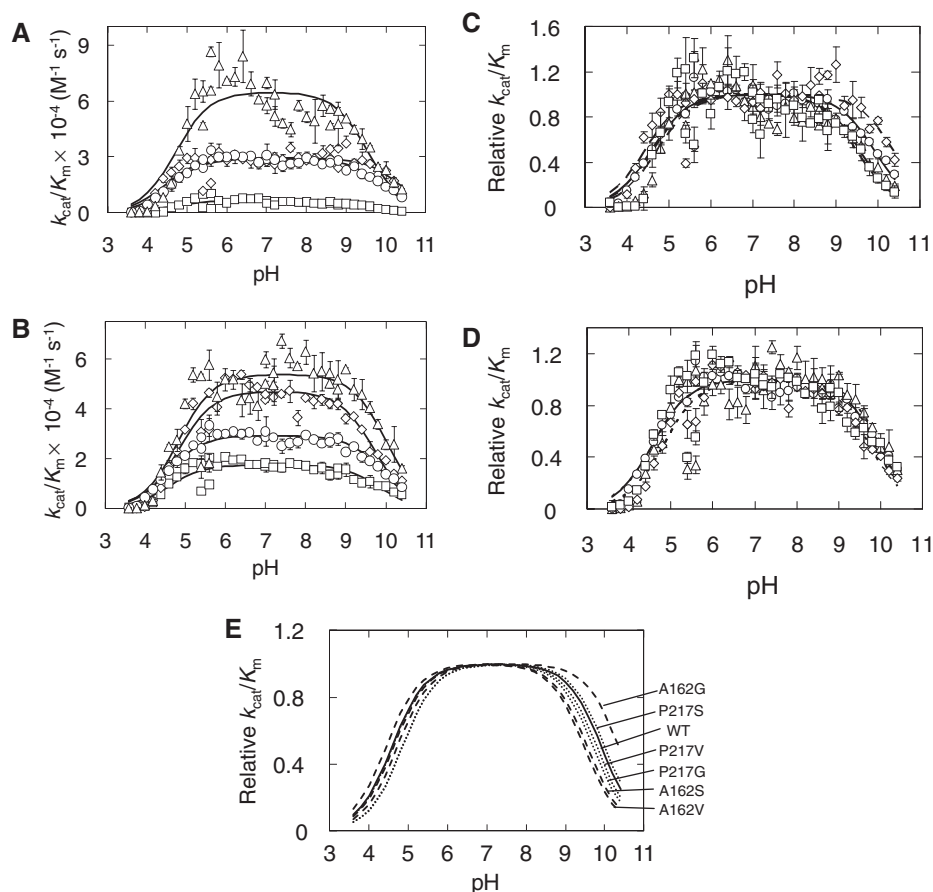


Fig. 5 Effects of pH on the MOCac-PLGL(Dpa)AR-hydrolysis activities of MMP-7 variants at 25°C. (A and C) Ala162 variants: WT (open circle); A162S (open triangle); A162V (open square); and A162G (open diamond). (B and D) Pro217 variants: WT (open circle); P217S (open triangle); P217V (open square); and P217G (open diamond). (C–E) Normalized profile of the pH dependence. Relative $k_{\text{cat}}/K_{\text{m}}$ is defined as the ratio of the $(k_{\text{cat}}/K_{\text{m}})_{\text{obs}}$ at the pH indicated to the $(k_{\text{cat}}/K_{\text{m}})_0$. Error bars indicate SD value. Solid, broken, and dotted lines were drawn by best-fitting the data to Equation (1).

Discussion

Estimation of a protein-bound water molecule as ionizable groups in the catalytic mechanism of MMP-7

The ionizable group responsible for pK_{e2} was assigned to Lys or Arg by thermodynamic analysis; however, no such residues are present in the active site (16). Regarding this, it should be noted that in α -chymotrypsin, the ionizable group for pK_{e2} of 8.5 was assigned to the α -amino group of N-terminal Ile residue, located far from the active site (29, 30). The α -amino group forms an ion pair with β -carboxyl group of Asp194, causing structural change required for catalysis (29, 30). In this study, all 19 MMP-7 variants, in which one of all Lys or Arg residues was replaced by Ala, retained activity (Table II), clearly indicating that neither Lys nor Arg residue is the ionizable group for pK_{e2} . Interestingly, R95A, K114A, K121A and K129A had reduced activity (2–15% of that of WT) despite that Arg95, Lys114, Lys121 and Lys129 are located far from the active site. They lie on the opposite side when MMP-7 is viewed with the active site at the centre (3).

It is difficult to demonstrate that a protein-bound water molecule as ionizable groups in the catalytic mechanism of enzyme. Solvent kinetic isotope effects (SKIEs), effects of light and heavy waters on the pH dependence of k_{cat}/K_m and k_{cat} of enzyme reaction, are effective to demonstrate the role of water molecule in catalysis, but they do not demonstrate a protein-bound water is an ionizable group. To address this issue, we made a combination of thermodynamic and site-directed mutagenesis analyses. In the thermodynamic analysis, the ΔH° value of deprotonation of water molecule was reported to be $55.80 \text{ kJ mol}^{-1}$ (31, 32), which is not much different from the ΔH° value of deprotonation for pK_{e2} of MMP-7 ($76 \pm 19 \text{ kJ mol}^{-1}$) (Fig. 4B). In the site-directed mutagenesis analysis, mutation of Ala162 and that of Pro217 do not abolish the activity (except for that of Ala162 into Pro) but affect it considerably (Tables II and III). Although there are no definitive results, our data support the possibility that a water molecule bound to the main-chain nitrogen of Ala162 (W1) or a water molecule bound to the main-chain carbonyl oxygen of Pro217 (W2) is the ionizable group for pK_{e2} . Interestingly, the activities of Ala162 variants were more reduced than those of Pro217 variants (Table II). The pH-dependence profiles of the k_{cat}/K_m values of Ala162 and Pro217 variants showed that at pH around the pK_{e2} value of WT (9.9), the profiles of the Ala162 variants were more different from that of WT than those of the Pro217 variants (Fig. 5). We speculate that the possibility of W1 as the ionizable group for pK_{e2} is higher than that of W2. However, further studies must be needed to clarify this possibility. It is also important to examine if a combination of thermodynamic analysis and site-directed mutagenesis analysis is useful to estimate ionizable groups in various enzyme activities.

Catalytic mechanism of MMP-7

The results presented in this study support the following catalytic mechanism of MMP-7, which we provided previously (16). In free enzyme, Glu198 is in its deprotonated state and W1 or W2 is in its unionized state. The geometries of Glu198, W1 and W2 are shown in Fig. 1D and E. The Michaelis complex is formed when the carbonyl oxygen of the scissile bond binds with the active-site zinc ion. The zinc ion polarizes the carbonyl group of the scissile bond. Glu198 accepts a proton from the zinc-bound water. The tetrahedral complex is formed when the ionized zinc-bound water attacks the carbonyl carbon of the scissile bond, and then stabilized by the interaction between the carbonyl oxygen and W1 or W2. The amino product is released when Glu198 transfers the proton to the nitrogen of the scissile bond.

Based on the crystal structure of MMP-3-sulphonamide inhibitor complex, the role of protein-bound water molecule in the catalytic mechanism of MMP-3 was proposed: the water is in the unionized state and stabilizes the tetrahedral intermediate by coordinating the carbonyl oxygen of the scissile bond of a substrate (33). In carboxypeptidase A, which is grouped in Clan MC of zinc metalloproteinase, the ionizable group for pK_{e1} of 7 was assigned to the active-site glutamate residue, and that for pK_{e2} of 10 was assigned to the zinc-bound water molecule (34). Although there is no definite evidence, we speculate that unionized W1 or W2 stabilizes the tetrahedral intermediate of MMP-7. Ala162 is in the fourth β -sheet (Ala162-Ala164), and Pro217 is in the Met-turn (Pro211-Gly222). It is interesting to note that the substitutions of Ala162 and Pro217 into Ser or Gly increased the activity, while those into Val, Leu and Lys decreased it. The replacement of Ala162 and Pro217 with bulky residues seems unfavourable for MMP-7 activity.

The catalytic importance of active-site glutamate residues corresponding to Glu198 of MMP-7 as a general base has been well recognized in other MMPs (35–38). However, it should be noted that Cha and Auld provided a theory that Glu198 of MMP-7 is catalytic important as a stabilizer of the tetrahedral complex rather than as a general base catalyst (13). In this study, the ionizable groups of MMP-7 were estimated to be Asp or Glu for pK_{e1} , and Glu198 in the active site was assigned. This suggests that Glu198 is in a deprotonated state for catalysis in free enzymes and accepts a proton from the zinc-bound water.

Catalytic Mechanism mechanism of Thermolysin

We examined the pH-dependence of k_{cat}/K_m of thermolysin at 15–45°C (Fig. 3B). By comparison with the ΔH° values of deprotonation of the side chains of free amino acids, the ionizable groups of thermolysin were assigned to Asp or Glu for pK_{e1} and Tyr, Cys or His for pK_{e2} . In thermolysin, there have been three mechanisms proposed for cleavage of peptides: (i) reaction catalysed by the thermolysin in which Glu143 is deprotonated and His231 is protonated (22); (ii) reaction catalysed by the thermolysin in which the zinc-bound

water is ionized and His231 is protonated (21); and (iii) reaction catalysed by the thermolysin in which the zinc-bound water is not ionized and His231 is not protonated (23). The third mechanism is called the reverse protonation catalytic mechanism. Our results support the first mechanism.

In conclusion, the present results of the combination of thermodynamic and site-directed mutagenesis analyses suggest a possibility that a protein-bound water molecule (specifically Ala162-bound water or Pro217-bound water) is the ionizable group responsible for pK_{e2} in the catalytic mechanism of MMP-7. They also indicate a possibility that the combination of thermodynamic and site-directed mutagenesis analyses is useful to estimate ionizable groups in enzyme activity.

Funding

Grants-in-Aid for Scientific Research, Japan Society for the Promotion of Science (Nos. 17380065 and 20380061) (to K.I., partial).

Conflict of interest

None declared.

References

1. Wilson, C.L. and Matrisian, L.M. (1996) Matrilysin: an epithelial matrix metalloproteinase with potentially novel functions. *Int. J. Biochem. Cell Biol.* **28**, 123–136
2. Woessner, J.F. Jr and Taplin, C.J. (1998) Purification and properties of a small latent matrix metalloproteinase of the rat uterus. *J. Biol. Chem.* **263**, 16918–16925
3. Browner, M.F., Smith, W.W., and Castelano, A.L. (1995) Matrilysin-inhibitor complexes: common themes among metalloproteinases. *Biochemistry* **34**, 6602–6610
4. Rawlings, N.D., Morton, F.R., Kok, C.Y., Kong, J., and Barrett, A.J. (2008) MEROPS: the peptidase database. *Nucleic Acids Res.* **36**, D320–D325
5. Muta, Y., Oneda, H., and Inouye, K. (2004) Inhibitory effects of alcohols on the activity of human matrix metalloproteinase 7 (matrilysin). *Biosci. Biotechnol. Biochem.* **68**, 2649–2652
6. Inouye, K., Shimada, T., and Yasukawa, K. (2007) Effects of neutral salts and alcohols on the activity of *Streptomyces caespitosus* neutral protease. *J. Biochem.* **142**, 317–324
7. Oneda, H. and Inouye, K. (2001) Interactions of human matrix metalloproteinase 7 (matrilysin) with the inhibitors thiorphan and R-94138. *J. Biochem.* **129**, 429–435
8. Muta, Y., Oyama, S., Umezawa, T., Shimada, M., and Inouye, K. (2004) Inhibitory effects of lignans on the activity of human matrix metalloproteinase 7 (matrilysin). *J. Agric. Food Chem.* **52**, 5888–5894
9. Oneda, H., Shiihara, M., and Inouye, K. (2003) Inhibitory effects of green tea catechins on the activity of human matrix metalloproteinase 7 (matrilysin). *J. Biochem.* **133**, 571–576
10. Miyake, T., Yasukawa, K., and Inouye, K. (2011) Analysis of the mechanism of inhibition of human matrix metalloproteinase 7 (MMP-7) activity by green tea catechins. *Biosci. Biotechnol. Biochem.* **75**, 1564–1569
11. Cha, J., Pedersen, M.V., and Auld, D.S. (1996) Metal and pH dependence of heptapeptide catalysis by human matrilysin. *Biochemistry* **35**, 15831–15838
12. Crabbe, T., Willenbrock, F., Eaton, D., Hynds, P., Carne, A.F., Murphy, G., and Docherty, A.J. (1992) Biochemical characterization of matrilysin. Activation conforms to the stepwise mechanisms proposed for other matrix metalloproteinases. *Biochemistry* **31**, 8500–8507
13. Cha, J. and Auld, D.S. (1997) Site-directed mutagenesis of the active site glutamate in human matrilysin: investigation of its role in catalysis. *Biochemistry* **36**, 16019–16024
14. Muta, Y., Oneda, H., and Inouye, K. (2005) Anomalous pH-dependence of the activity of human matrilysin (matrix metalloproteinase-7) as revealed by nitration and amination of its tyrosine residues. *Biochem. J.* **386**, 263–270
15. Muta, Y. and Inouye, K. (2011) Tyr219 of human matrix metalloproteinase 7 (MMP-7) is not critical for catalytic activity, but is involved in the broad pH-dependence of the activity. *J. Biochem.* **150**, 183–188
16. Takeharu, H., Yasukawa, K., and Inouye, K. (2011) Thermodynamic analysis of ionizable groups involved in the catalytic mechanism of human matrix metalloproteinase 7 (MMP-7). *Biochim. Biophys. Acta* **1814**, 1940–1946
17. Betz, M., Huxley, P., Davies, S.J., Mushtaq, Y., Pieper, M., Tschesche, H., Bode, W., and Gomis-Rüth, F.X. (1997) 1.8-Å crystal structure of the catalytic domain of human neutrophil collagenase (matrix metalloproteinase-8) complexed with a peptidomimetic hydroxamate primed-side inhibitor with a distinct selectivity profile. *Eur. J. Biochem.* **247**, 356–363
18. Inouye, K. (2003) *Thermolysin in Handbook of Food Enzymology*. (Whitaker, J.R., Voragen, A.G.J., and Wong, D.W.S., eds.), pp. 1019–1028, Marcel Dekker, New York
19. Kusano, M., Yasukawa, K., Hashida, Y., and Inouye, K. (2006) Engineering of the pH-dependence of thermolysin activity as examined by site-directed mutagenesis of Asn112 located at the active site of thermolysin. *J. Biochem.* **139**, 1017–1023
20. Tatsumi, C., Hashida, Y., Yasukawa, K., and Inouye, K. (2007) Effects of site-directed mutagenesis of the surface residues Gln128 and Gln225 of thermolysin on its catalytic activity. *J. Biochem.* **141**, 835–842
21. Kuzuya, K. and Inouye, K. (2001) Effects of cobalt-substitution of the active zinc ion in thermolysin on its activity and active-site microenvironment. *J. Biochem.* **130**, 783–788
22. Matthews, B.W. (1988) Structural basis of the action of thermolysin and related zinc peptidases. *Acc. Chem. Res.* **21**, 333–340
23. Mock, W.L. and Stanford, D.J. (1996) Arazoformyl dipeptides substrate for thermolysin. Confirmation of a reverse protonation catalytic mechanism. *Biochemistry* **35**, 7369–7377
24. Knight, C.G., Willenbrock, F., and Murphy, G. (1992) A novel coumarin-labelled peptide for sensitive continuous assays of the matrix metalloproteinase. *FEBS Lett.* **296**, 263–266
25. Muta, Y., Yasui, N., Matsumiya, Y., Kubo, M., and Inouye, K. (2010) Expression in *Escherichia coli*, refolding, and purification of the recombinant mature form of human matrix metalloproteinase 7 (MMP-7). *Biosci. Biotechnol. Biochem.* **74**, 2515–2517

26. Oneda, H. and Inouye, K. (1999) Refolding and recovery of recombinant human matrix metalloproteinase 7 (matrilysin) from inclusion bodies expressed by *Escherichia coli*. *J. Biochem.* **126**, 905–911
27. Oneda, H. and Inouye, K. (2000) Effects of dimethyl sulfoxide, temperature, and sodium chloride on the activity of human matrix metalloproteinase 7 (Matrilysin). *J. Biochem.* **128**, 785–791
28. Laemmli, U.K. (1970) Cleavage of structural proteins during the assembly of the head of bacteriophage T4. *Nature* **227**, 680–685
29. Oppenheimer, H.L., Labouesse, B., and Hess, G.P. (1966) Implication of an ionizing group in the control of conformation and activity of chymotrypsin. *J. Biol. Chem.* **241**, 2720–2730
30. Sigler, P.B., Blow, D.M., Matthews, B.W., and Henderson, R. (1968) Structure of crystalline α -chymotrypsin II. A preliminary report including a hypothesis for the activation mechanism. *J. Mol. Biol.* **35**, 143–164
31. Hale, J.D., Izatt, R.M., and Christensen, J.J. (1963) A calorimetric study of the heat of ionization of water at 25°. *J. Phys. Chem.* **67**, 2605–2608
32. Vanderzee, C.E. and Swanson, J.A. (1963) The heat of ionization of water. *J. Phys. Chem.* **67**, 2608–2612
33. Pelmenchikov, V. and Siegbahn, P.E. (2002) Catalytic mechanism of matrix metalloproteinases: two-layered ONIOM study. *Inorg. Chem.* **41**, 5659–5666
34. Zhang, K. and Auld, D.S. (1995) Structure of binary and ternary complexes of zinc and cobalt carboxypeptidase A as determined by X-ray absorption fine structure. *Biochemistry* **34**, 16306–16312
35. Windsor, L.J., Bodden, M.K., Birkedal-Hansen, B., Engler, J.A., and Birkedal-Hansen, H. (1994) Mutational analysis of residues in and around the active site of human fibroblast-type collagenase. *J. Biol. Chem.* **269**, 26201–26207
36. Arza, B., De Maeyer, M., Félez, J., Collen, D., and Lijnen, H.R. (2001) Critical role of glutamic acid 202 in the enzyme activity of stromelysin-1 (MMP-3). *Eur. J. Biochem.* **268**, 826–831
37. Rowsell, S., Hawtin, P., Minshull, C.A., Jepson, H., Brockbank, S.M., Barratt, D.G., Slater, A.M., McPheat, W.L., Waterson, D., Henney, A.M., and Pauptit, R.A. (2002) Crystal structure of human MMP9 in complex with a reverse hydroxamate inhibitor. *J. Mol. Biol.* **319**, 173–181
38. Tallant, C., Marrero, A., and Gomis-Rüth, F.X. (2010) Matrix metalloproteinases: Fold and function of their catalytic domains. *Biochim. Biophys. Acta* **1803**, 20–28